






Article

Can Crude Oil Exploration Influence the Phytochemicals and Bioactivity of Medicinal Plants? A Case of Nigerian *Vernonia amygdalina* and *Ocimum gratissimum*

Oluwatofunmilayo A. Diyaolu ^{1,*}, Emmanuel T. Oluwabusola ¹, Alfred F. Attah ², Eric O. Olori ³, Adeshola A. Fagbemi ⁴, Gagan Preet ¹, Sylvia Soldatou ¹, Jones O. Moody ⁵, Marcel Jaspars ¹ and Rainer Ebel ^{1,*}

¹ Marine Biodiscovery Centre, Department of Chemistry, University of Aberdeen, Aberdeen AB24 3UE, UK

² Department of Pharmacognosy and Drug Development, Faculty of Pharmaceutical Sciences, University of Ilorin, Ilorin 240003, Nigeria

³ Department of Pharmaceutical Chemistry, Faculty of Pharmacy, University of Ibadan, Ibadan 200005, Nigeria

⁴ Department of Pharmaceutical Chemistry, Faculty of Pharmacy, Lead City University, Ibadan 200255, Nigeria

⁵ Department of Pharmacognosy, Faculty of Pharmacy, University of Ibadan, Ibadan 200005, Nigeria

* Correspondence: r01oad17@abdn.ac.uk (O.A.D.); r.ebel@abdn.ac.uk (R.E.)

Abstract: The Nigerian Niger-Delta crude oil exploration often results in spills that affect indigenous medicinal plant biodiversity, likely changing the phytochemical profile of surviving species, their bioactivity or toxicity. In crude oil-rich Kokori and crude oil-free Abraka, classic examples of indigenous plants occupying the medicine-food interface include *Vernonia amygdalina* (VAL) and *Ocimum gratissimum* leaves (OGL). These plants are frequently utilised during pregnancy and in anaemia. To date, no scientific investigation has been reported on the potential changes to the phytochemical or bioactivity of the study plants. To discuss the similarities and dissimilarities in antisickling bioactivity and phytochemicals in VAL and OGL collected from Kokori (VAL-KK and OGL-KK) and Abraka (VAL-AB and OGL-AB), in silico, in vitro and comparative UPLC-QTOF-MS analysis was performed. Nine unique compounds were identified in OGL-KK, which have never been reported in the literature, while differences in antisickling potentials were observed in VAL-KK, OGL-KK and, VAL-AB, OGL-AB. Our findings show that VAL-AB and OGL-AB are richer and more diverse in phytochemicals and displayed a slightly higher antisickling activity than VAL-KK and OGL-KK. Ligand-based pharmacophore modelling was performed to understand the potential compounds better; this study may provide a basis for explaining the effect of crude oil spills on secondary metabolites and a reference for further research.

Keywords: *Vernonia amygdalina* leaves; *Ocimum gratissimum* leaves; UPLC-QTOF-MS; sickle cell anaemia; molecular docking; metabolomics; pharmacophore; drug design; in silico



Citation: Diyaolu, O.A.; Oluwabusola, E.T.; Attah, A.F.; Olori, E.O.; Fagbemi, A.A.; Preet, G.; Soldatou, S.; Moody, J.O.; Jaspars, M.; Ebel, R. Can Crude Oil Exploration Influence the Phytochemicals and Bioactivity of Medicinal Plants? A Case of Nigerian *Vernonia amygdalina* and *Ocimum gratissimum*. *Molecules* **2022**, *27*, 8372. <https://doi.org/10.3390/molecules27238372>

Academic Editor: David Barker

Received: 19 October 2022

Accepted: 27 November 2022

Published: 30 November 2022

Publisher's Note: MDPI stays neutral with regard to jurisdictional claims in published maps and institutional affiliations.



Copyright: © 2022 by the authors. Licensee MDPI, Basel, Switzerland. This article is an open access article distributed under the terms and conditions of the Creative Commons Attribution (CC BY) license (<https://creativecommons.org/licenses/by/4.0/>).

1. Introduction

The World Health Organisation has reported that no less than 80% of the African populace relies on medicinal herbs for their essential healthcare needs. However, ethnomedicinal plant use is partly tied to poverty, cultural resistance and poor accessibility to modern healthcare [1]. For example, *Vernonia amygdalina* leaves (VAL) and *Ocimum gratissimum* leaves (OGL) are commonly used to manage sickle cell disease (SCD) [2]. The leaves are macerated in an aqueous or alcoholic medium, and the extracted juice is administered [3,4]. *Vernonia amygdalina*, commonly known as “bitter leaf,” is a small shrub with dark green leaves and rough bark [5], mainly growing in tropical Africa but domesticated in many parts of West Africa. *Ocimum gratissimum*, also known as African basil, is cultivated in many gardens around village huts in Nigeria for medicinal and culinary uses [6]. Both VAL and OGL contain a myriad of phytochemicals. More than forty compounds belonging to several classes of secondary metabolites with differing bioactivities have been isolated

and characterised from VAL and OGL. The isolated compounds have shown a broad spectrum of activities ranging from antifeedant [7], antischistosomal [8], antiplasmodial [9], antioxidant [10], anti-inflammatory [11] and anticancer activities [12].

VAL and OGL are both found in nature close to rivers and lakes. They can thrive on all soil types but grow better on humus-rich soils. However, they can withstand drought and other harsh conditions because they have continuously survived the massive crude oil spillage in Kokori Delta State, Nigeria. Kokori is crude oil-rich and one such community in Delta State where crude oil exploration and effluent release are common, and these activities have led to the death of many medicinal plants. However, VAL and OGL have survived with a possibility of an alteration of the phytochemical profile. The indigenes of this region continue to use these plants for medicinal purposes without considering the potentially detrimental effects this may have. Although there have been reports on the heavy metal content and proximate analysis of VAL and OGL in crude oil-rich communities in Delta state [13], there has been a lack of profound reports on the comprehensive screening and identification of the phytochemicals of VAL and OGL surviving crude oil-contaminated environments like Kokori. The question, therefore, arises whether VAL and OGL produce different and potentially new chemical entities as they adapt to the environmental stress caused by continuous crude oil exploration. Furthermore, not all communities in Delta state are crude oil-rich; an example of a nearby “crude oil-free” community is Abraka [14].

Sickle-cell disease is a multisystem disease accompanied by bouts of acute illness and continuing organ damage restitution. It is one of the world’s most common critical monogenic disorders. The prevalence of the disease has been predominantly reported in resource-restricted countries, and about 80% of SCD incidences eventuate in sub-Saharan Africa. The haemoglobin biophysics and eugenics of the disease have been studied in detail and have helped the understanding of other molecular illnesses. Nevertheless, clinical management of sickle-cell disease is still elementary. Although some evidence confirms support for the utilisation of blood transfusion and hydroxycarbamide, no drugs have been established that explicitly target the pathophysiology of this disease [15]. An anomaly characterises sickle cell anaemia resulting from SCD in the haemoglobin (haemoglobin S, HbS) carrying oxygenated blood due to a point mutation substituting a charged and hydrophilic glutamic acid with a hydrophobic valine at position 6 of the β -globin polypeptide chain [16]. Under deoxygenation circumstances (low oxygen tension), the mutant HbS polymerises within the red blood cells (RBCs) into a rigid gel and then into fibres causing a decrease in red blood cells (RBC) deformability. HbS polymerisation occurring within the erythrocytes prompts a modification in the available frame from a typical spheroidal form into disfigured shapes, with some mimicking a sickle [17]. The HbS molecule plays a central role in disease development. Thus, efforts to develop new leads for SCD management should target the inhibition of HbS polymerisation. For example, the recently FDA-approved voxelotor is a covalent modifier of the HbS molecule and acts as an allosteric modulator preserving the haemoglobin molecule in its non-aggregating R-conformer [18].

Normal haemoglobin has a quaternary structure as a tetrameric protein constituent with two α and two β -chains individually and covalently connected to a heme molecule. In the α and β -chains of haemoglobin, there are 141 and 146 amino acids, respectively [19]. Although interactions between several haemoglobin tetrameric units may result in polymerisation, such aggregates are usually unstable under typical physiologic conditions. In homozygous SS patients, the beta-chains contain valine instead of a glutamic acid at position 6, thus enabling it to form hydrophobic connections with identical uncharged hydrophobic units like Phe85 and Leu88 of the adjacent β -globin chain. These connections are secondarily stabilised by other contacts involving segments of the haemoglobin molecule that are remote from the E6V mutation. These contacts form the basis for HbS polymerisation and establish the SCD symptom complex. Normal red blood cells are flexible, can wring through tight capillary junctions and have a lifespan of 90 to 120 days. They circulate across arteries, veins, and tiny capillaries during this period, travelling about 500 km [20]. However, due to the stiffening nature of sickled RBCs, they cannot readily

change shape, and the strain of squeezing through tight vascular junctions imparts their tendency to haemolyse; as a result, sickle RBCs have a short lifespan of 10 to 20 days, thus causing anaemia. Only a handful of drugs with significant side effects, including hydroxyurea [21], L-glutamine [22], crizanlizumab [23], and voxelotor [24] are available for managing SCD to date. Hence, there is an urgent need to identify new drugs, particularly plant-derived agents, that are non-toxic and effectively act at various steps of the sickle cell disease pathophysiologic cascade.

The findings in this paper report for the first time the similarities and differences in the antisickling potential and phytochemical profile of *Vernonia amygdalina* (VAL) and *Ocimum gratissimum* (OGL) leaves collected from an explored crude oil-rich Kokori and the crude oil-free species from Abraka in Delta state of Nigeria. To reveal the diversity of the metabolites, untargeted metabolomics analysis was performed to profile diverse classes of the metabolites and compare the overall small-molecule metabolites present in the samples. In order to achieve this, a combination of UPLC separation, QTOF-MS detection, and multivariate statistical evaluation (principal component analysis, PCA) was used to profile the four types of leaf samples. Polymerisation inhibition and sickling reversal tests were used as assay methods to evaluate the anti-sickling activities of the different plants' extracts. In addition, *in silico* molecular studies were carried out on the compounds isolated from the crude extracts. Our data might provide a compelling basis for further scientific research in Nigeria to investigate the effect of crude-oil exploration-induced environmental stress on the chemical profile, efficacy and safety of commonly consumed medicinal plants in populated rural settings. Findings from such in-depth and elaborate studies could trigger appropriate policy reviews that will mitigate against any possible loss of important plant biodiversity and improve or safeguard the health of the local populations.

2. Materials and Methods

2.1. Materials and Reagents

VAL and OGL were collected in March 2021 from six different sites; three randomly selected locations within crude oil-rich Kokori and the other three collected from random locations within the crude oil-free Abraka community (Table 1). The plant samples were collected in April 2017 during the dry season, just before the onset of the rainy season. The identities of *Vernonia amygdalina* and *Ocimum gratissimum* leaves were confirmed and authenticated at the Forest Herbarium Ibadan, Nigeria, where voucher specimens were deposited (FHI 10,988 and 109,823). Milli-Q water, methanol and acetonitrile (Rathburn Chemicals Ltd., Walkerburn, UK) were used for the UPLC-MS. Formic acid for UPLC was purchased from Fisher Scientific Ltd., Leicestershire, UK. All chemicals used were of analytical grade. Standard compounds rutin, kaempferol, caffeic acid, catechin, reserpine, eugenol, quercetin, luteolin, isorhamnetin, and oleic acid was purchased from the Nigerian Agency for Food and Drug Administration and Control (Lagos, Nigeria).

Table 1. List of tested samples from Kokori and Abraka, Delta State, Nigeria. Legend: VAL, *Vernonia amygdalina* leaf; OGL, *Ocimum gratissimum* leaf.

# Species	Sample No.	Community	Source	Coordinates
VAL	1	Abraka	Oria	5°45' N 6°15' E
	2	Abraka	Urhuovie	5°47' N 6°15' E
	3	Abraka	Ajalom	5°47' N 6°15' E
	4	Kokori	Egbo	5°38' N 6°04' E
	5	Kokori	Kokori	5°38' N 6°15' E
	6	Kokori	Samagidi	5°38' N 6°22' E

Table 1. Cont.

# Species	Sample No.	Community	Source	Coordinates
OGL	7	Abraka	Oria	5°45' N 6°15' E
	8	Abraka	Urhuovie	5°47' N 6°15' E
	9	Abraka	Ajalom	5°47' N 6°15' E
	10	Kokori	Egbo	5°38' N 6°04' E
	11	Kokori	Kokori	5°38' N 6°15' E
	12	Kokori	Samagidi	5°38' N 6°22' E

Plant samples were collected in April 2017, towards the end of the dry season.

2.2. Sample Preparation and Extraction

Debris and stalks were removed from the leaves before air-drying, weighed (1.0 g) and extracted in 70% ethanol (1.0 L) for 72 h with occasional stirring. After being filtered, the extraction solution was concentrated using a rotary evaporator (IKA, UK) at 40 °C under reduced pressure. The extracts were further concentrated by freeze-drying and stored at −20 °C for further investigation and analysis.

2.3. Mass Spectral Data Acquisition

Extracts were dissolved in methanol at a final concentration of 0.1 mg/mL, centrifuged and injected onto a Phenomenex Kinetex XB-C18 (2.6 mM, 100 × 2.1 mm) column. Samples were analysed using a Bruker maXisII electrospray ionisation quadrupole time-of-flight (ESI-qToF) mass spectrometer coupled with an Agilent 1290 UHPLC system. The elution conditions were 5% ACN + 0.1% FA to 100% ACN + 0.1% FA in 15 min. Mass range was set to m/z 100–2000. The positive and negative mode conditions were as follows: capillary voltage 4.5 kV, nebuliser gas 4.5 bar, dry gas 12.0 L/min, and dry temperature of 250 °C. MS/MS experiments were conducted under Auto MS/MS scan mode with no step collision. The external reference lock mass (sodium formate) was infused at a constant flow of 0.1 mL/h.

2.4. Phytochemical Analysis of Metabolites of VAL and OGL Using UNIFI Platform

The UNIFI 1.7.0 software (Waters, Manchester, UK) [25], Ref. [26] was first used to identify the chemical compounds present in all the plant samples; the MS raw data (.d) was automatically screened using an established streamlined workflow. The parameters used were fine tuned as follows: minimum peak area was set to 200 for 2D peak detection, peak intensities for low and high energy were set above 1000 and 200 counts consecutively for 3D peak detection; 5 ppm for mass error, and 0.1 min retention time to match the standard reference. The speculated fragments were recognised as the matching compounds. Both negative and positive adducts were selected in the analysis. Reserpine was used as the reference compound, $[M + H]^+$ 609.6773 was used as the positive ion and $[M - H]^-$ 607.6617 was the negative ion. Phytochemicals were further verified by comparing generated fragmentation patterns with characteristic MS fragmentation patterns in published literature and comparing reference compounds with retention time. The investigation of the phytochemicals was carried out systematically. In addition to the in-built Waters UNIFI Traditional Medicine Library, the following databases were used to source chemical information for the compounds: ChemSpider, Pubmed, Pubchem, Reaxys, and Web of Science. These aided the formation of a self-built database of phytochemicals isolated from VAL and OGL.

2.5. Metabolomic Analysis

The crude extracts' obtained HPLC-MS/MS data were converted from data analysis (.d) to .mzXML file format using MSConvert software [27]. The .mzXML files were further processed using MZmine software [28]. The following parameter modules were used: mass

detection (RT 2.5–35 min, centroid); chromatogram builder (MS level 1; minimum height 1.0×10^4 ; minimum time 0.5 min; m/z tolerance 10 ppm); deconvolution of the spectra (Algorithm Savitzky-Golay); isotopic peaks grouper (m/z tolerance 10 ppm; retention time (RT) tolerance 0.1 min); duplicate peak filtering; smoothing; data alignment (Join aligner; m/z tolerance 10 ppm; RT tolerance 0.5 min); gap-filling (intensity tolerance 20%; m/z tolerance 10 ppm, RT tolerance 0.5 min); and peak filtering range (0.00–0.5 min). After processing the data, peaks with matching RT and m/z in different samples were regarded as belonging to the same component. Furthermore, multivariate statistical analysis was performed. Firstly, principal component analysis (PCA) showed pattern recognition and maximum variation to obtain the overview, classification and variables that emerge as significant to get the maximum separation between the crude oil-contaminated VAL and OGL and the crude oil-free VAL and OGL groups and explore the potential phytochemicals that contribute to the differences. Then, S-plots were created to provide visualisation of the OPLS-DA to enable model elucidation. Simultaneously, the use of variable importance for the projection (VIP) helped screen the different phytochemicals, and compounds with VIP values >1.0 and p -value below 0.05 were considered significant [26]. Additionally, permutation testing was performed to indicate the R^2/Q^2 values that could indicate statistical significance [29]. Finally, Simca 15.0 software (Umetrics, Malmö, Sweden) was used to show the analysis results [30].

2.6. Blood Sample Collection and Ethical Approval

Blood samples from sickle cell anaemia (HbSS) patients were collected from the University College Hospital, Ibadan, Nigeria. 4 mL of blood samples were collected by venipuncture directly into ethylene diamine tetra acetic acid (EDTA) anticoagulant bottles. The blood samples were centrifuged and washed with phosphate-buffered saline pH: 7.4 (PBS: 1.3 M NaCl, 0.07 M Na_2HPO_4 and 0.03 M NaH_2PO_4) at 3000 rpm for 5 min. All experimental protocols were conducted and compliant with the ethical approval of the University of Ilorin Ethics Committee Guidelines and internationally accepted principles as found in US guidelines (NIH publication #85-23, revised in 1985).

2.7. In Vitro Sickling Reversal Assay

A sickling reversal test was carried out using the method previously described in the literature [31]. 1 mL of HbS blood collected was added to 5 mL of phosphate-buffered saline (PBS- pH 7.4) in a centrifuge tube. The content was centrifuged at 3000 rpm for 15 min. The supernatant was discarded, and the process was repeated to obtain a clear supernatant. The red blood cells were re-suspended with 1 mL of PBS and used for the test. 40 μL of the washed red blood cells were pipetted into a clean Eppendorf tube using a micropipette. 30 μL of PBS was added to the Eppendorf tube containing the washed blood. 800 μL of freshly prepared 2% sodium metabisulfite was added and incubated in a thermostated water bath at 37 °C for 1 h. 200 μL of PBS was added after the initial incubation period and incubated for another 1 h at 37 °C. 10 μL of the incubated cells were transferred onto a hemocytometer. The cells were counted at five zones using a differential counter (control); this process was repeated by substituting the 200 μL of distilled water added after the first incubation with 200 μL each of the extracts at three different concentrations (10, 5 and 2 mg/mL). The cells were classified as normal or sickle using visual inspection of their shapes.

Calculation:

Normal cells = Biconcave or disk-like shapes

Sickle cells = star-like or wrinkled shapes

$$\% \text{ Sickled} = \frac{\text{Number of sickle cells}}{\text{Total number of cells}} \times 100$$

$$\% \text{ Reversal} = \frac{(\% \text{ sickled cells control} - \% \text{ sickled cells test})}{\% \text{ sickled cells control}} \times 100$$

2.8. Isolation of Secondary Metabolites

1D and 2D NMR data were recorded on Bruker AVANCE II 600 MHz and 400 MHz spectrometers. The spectra were obtained at 300 K in CD₃OD. The CD₃OD solvent signals (¹H; 3.31 ppm and ¹³C; 49.1 ppm) were used to reference the spectra. HR-ESI-MS data were obtained using an Agilent 6540 HR-ESI-TOF-MS coupled to an Agilent 1200 HPLC system. Fractionations were performed on a solid-phase extraction column using C18-E (Phenomenex, 55 µm, 70 Å, 2 g/12 mL, Giga tubes). Fractions were further purified on an Agilent 1200 semipreparative HPLC system equipped with a binary pump, photodiode array detector (DAD)22, Waters Sunfire reversed-phase column C18 (5 µm, 10 × 250 mm), and Agilent Zorbax C18 (5 µm, 9.4 × 250 mm), and a mobile phase gradient system between 95:5% and 20:80% (H₂O/MeOH).

2.9. Molecular Docking

The crystal structure of deoxyhemoglobin S (PDB ID: 2HBS) [32] and P-selectin (PDB ID: 1G1S) [33] was obtained from the protein data bank (<https://www.rcsb.org/>, accessed: 28 September 2022). Prior to protein preparation, heteroatoms and co-crystallised ligand were removed. The dock prep module of the UCSF chimera software program (University of California, Oakland, CA, USA) [34] was used for protein preparation. Briefly, solvent molecules co-crystallised with the proteins were deleted; hydrogen atoms were added to the protein. In addition, the Dunbrack 2010 rotamer library [35] was used to predict the missing side chains, and charges were defined using AM1-BCC. The protein structure was minimised with the AMBERff14SB force field. The minimisation parameters include 300 steepest descent steps at a step size of 0.02 Å, conjugate gradient steps at 10 and an update interval of 10. Subsequently, the protein was loaded on PYRX for molecular docking [36]. The ligand; vernodalol was downloaded from pubchem.ncbi.nlm.nih.gov/ accessed on 28 September 2022) with Pubchem ID 442318. The structure of lasiopulide was identified from [37] and constructed using ChemDraw (RRID: SCR_016768). The ligands were imported to PYRX, and the docking parameters are shown in the Table 2:

Table 2. Docking parameters.

Target Name	PDB Code	Dimensions (Å)	Centre
deoxyhemoglobin S	2HBS	X: 24.4838; Y: 26.6805; Z: 25.0000	X: 7.5857; Y: 11.1820; Z: 28.1205
P-selectin	1G1S	X: 34.1555; Y: 21.0892; Z: 25.0000	X: 43.7339; Y: 85.8462 Z: 48.1365

2.10. 3D Pharmacophore Model Generation

LigandScout by Inte Ligand, Expert software (Wolber and Langer), Vienna, Austria, Europe [38] (license key: 44427459425915253797) was used to generate a 3D pharmacophore model. Espresso algorithm was used to generate ligand-based pharmacophore. The generated pharmacophore model compatibility with the pharmacophore hypothesis was created using default settings for LigandScout. Relative Pharmacophore-Fit scoring function, Merged feature pharmacophore type and feature tolerance scale factor was set to 1.0 for Ligand-Based Pharmacophore creation. The best model was selected from the 10 generated models.

2.11. Statistical Analysis

The results obtained from all experiments were performed in triplicates and expressed as the mean ± SEM. The statistical significance of the means differences was established by analysis of variance (ANOVA) with Duncan's post hoc tests. *p*-values < 0.05 were considered statistically significant.

3. Results and Discussion

3.1. Identification of Phytochemicals from VAL and OGL Based on the UNIFI Platform

The screening analysis revealed that 70 compounds were identified or tentatively characterised in ESI⁺ and ESI⁻ mode from VAL and OGL from crude oil-rich Kokori and crude oil-free Araka. Seven shared constituents were identified in VAL and OGL from both communities (VAL-AB, OGL-AB, VAL-KK and OGL-KK); 6 constituents were exclusively identified in VAL-KK and OGL-KK. More specifically, 34 compounds were characterised from VAL-AB, 20 from VAL-KK, 39 from OGL-AB and 21 from OGL-KK. (Table S3). Samples obtained from crude oil-free Araka (VAL-AB and OGL-AB) displayed richer chemical profiles with various structural patterns, including flavonoids, glycosides, organic acids, iridoids, saponins and steroids, compared to samples collected from crude oil-spill Kokori (VAL-KK and OGL-KK). The base peak chromatograms marked with the number of compounds are shown in Figures S1 and S2. The structures of the phytochemicals are summarised in Figure 1.

(a) Organic acids and organic acid esters

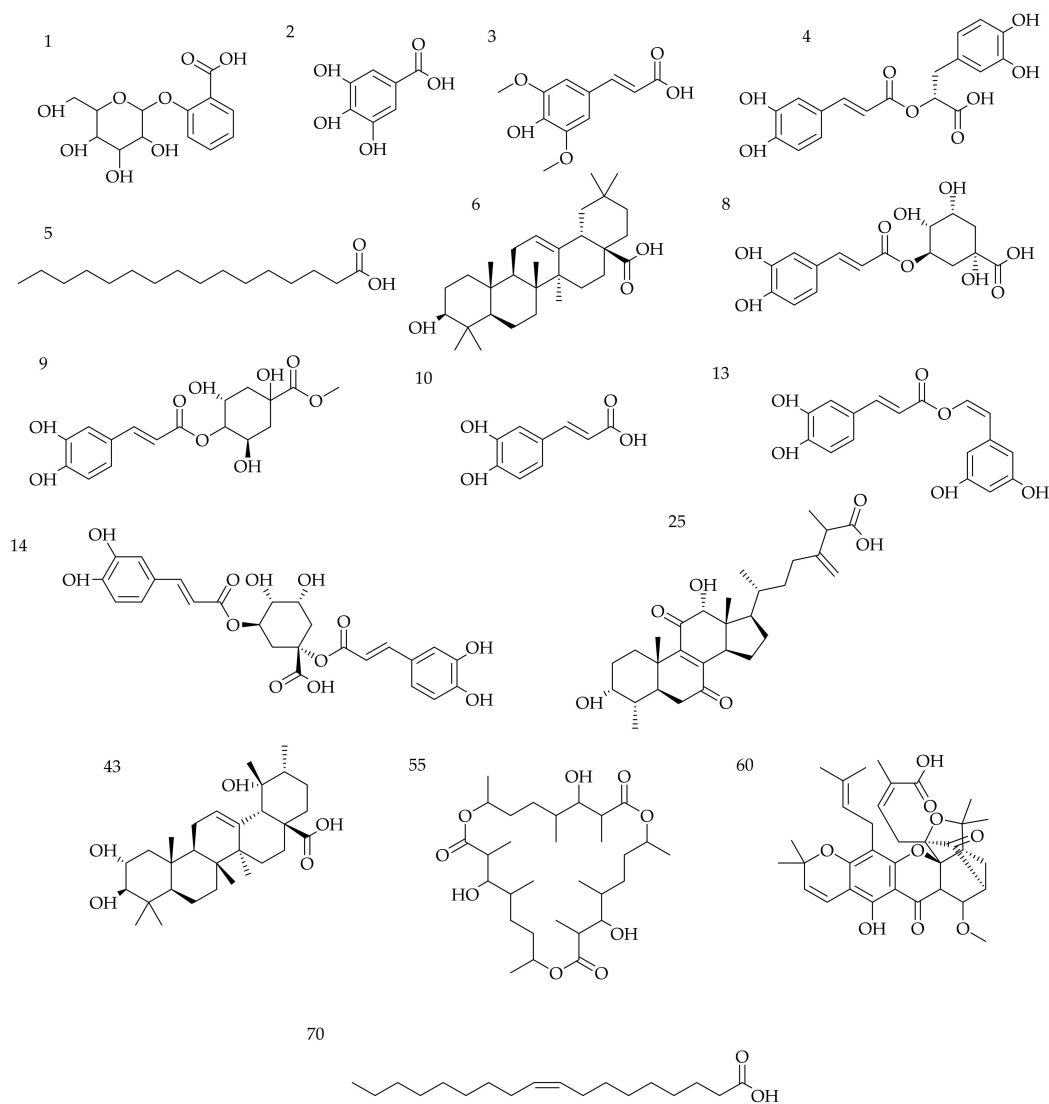


Figure 1. Cont.

(b) Flavonoids

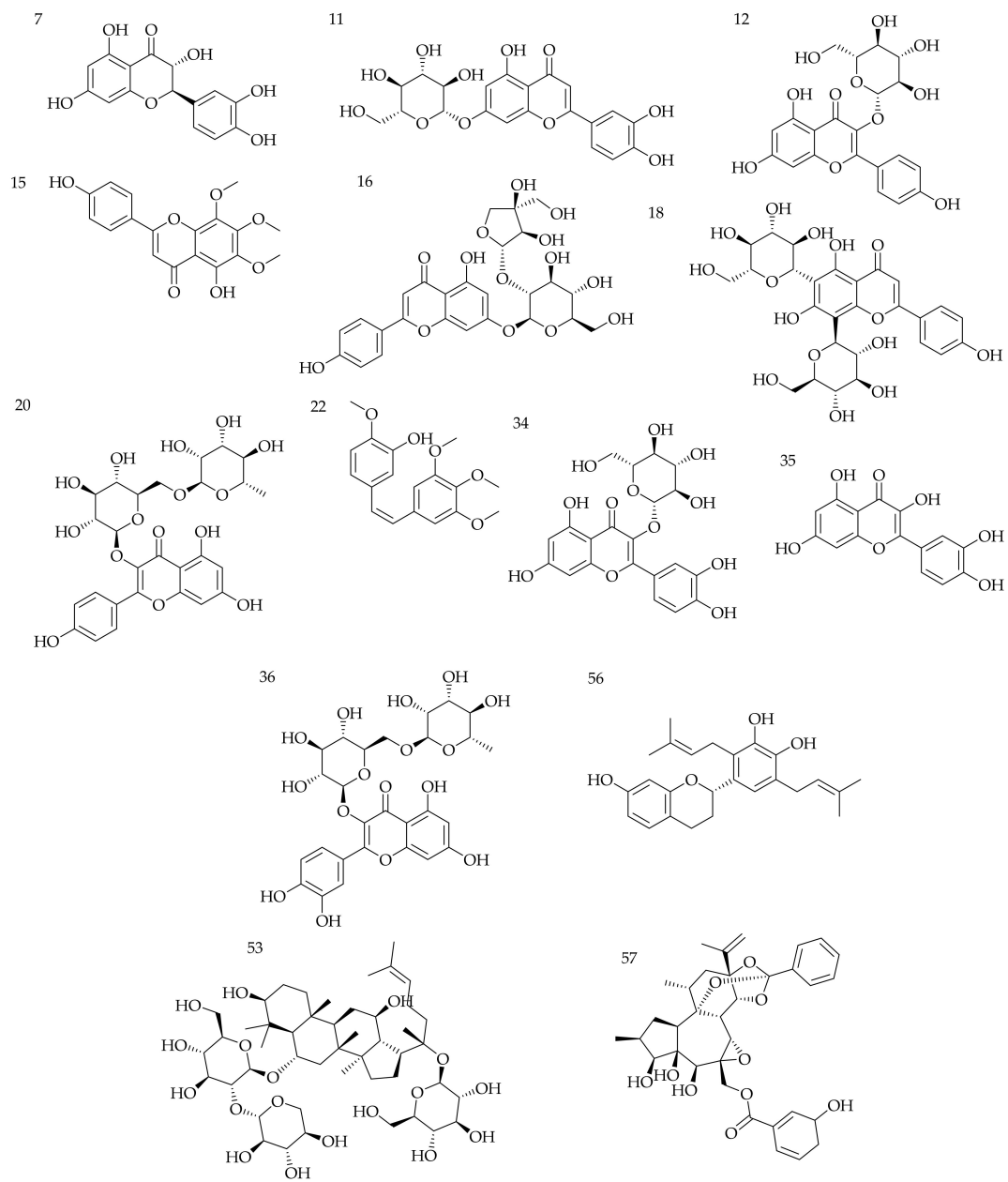


Figure 1. Cont.

(c) Terpenes

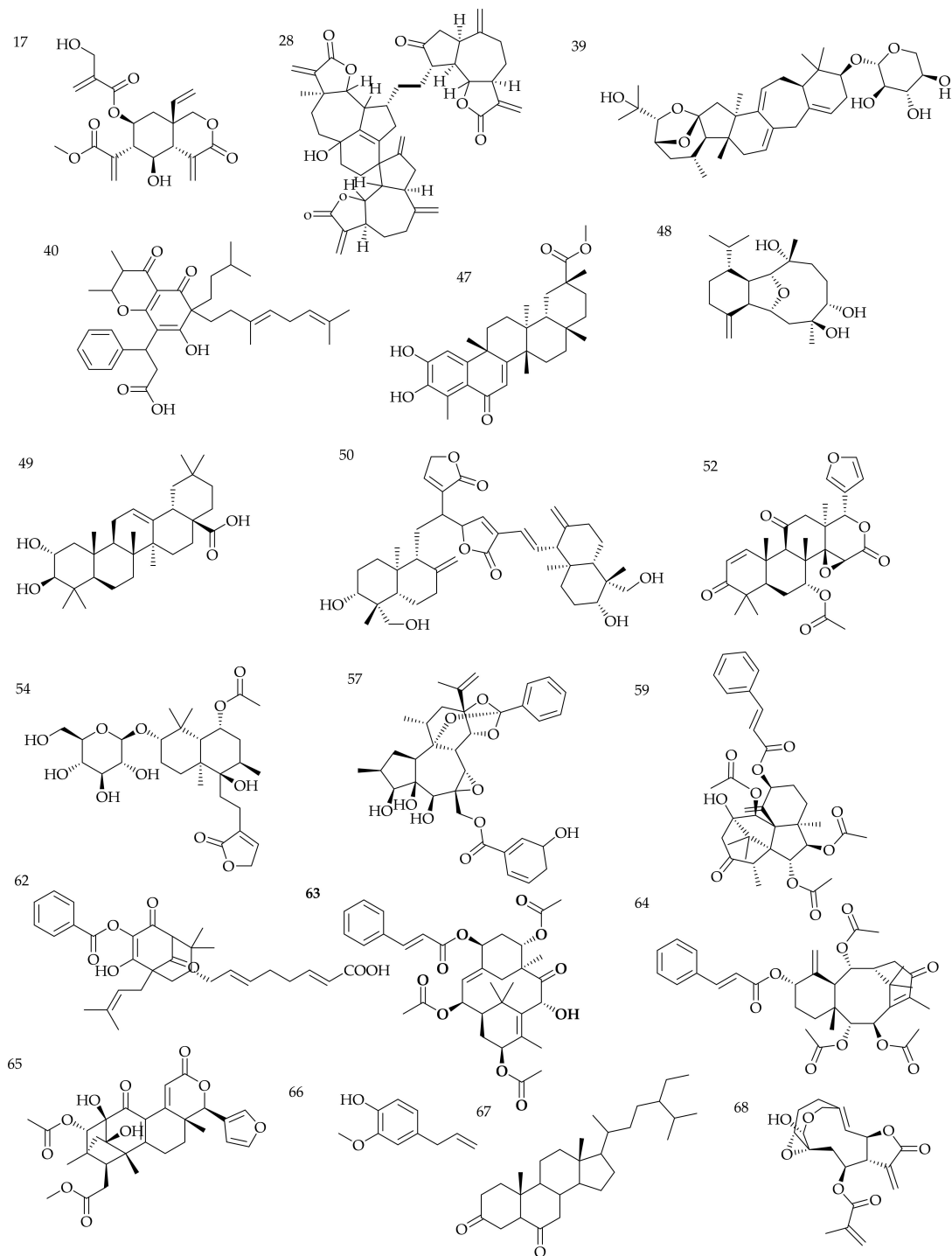


Figure 1. Cont.

(d) Others

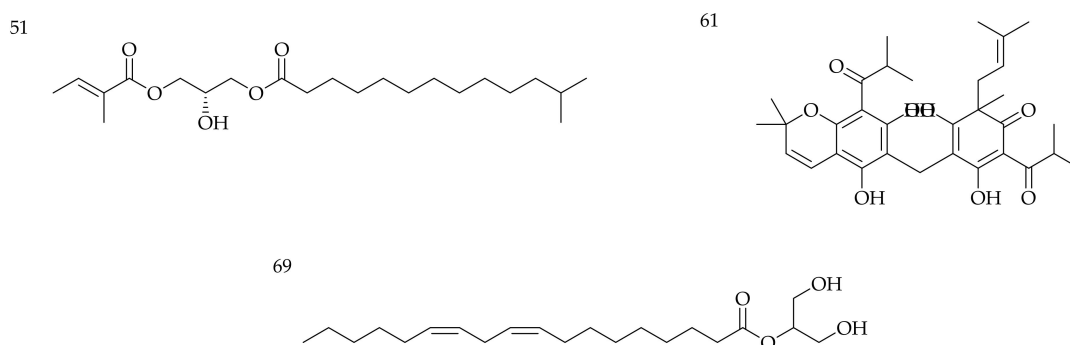


Figure 1. (a–d) Chemical structures of compounds identified in VAL and OGL from Kokori and Abraka. (a) organic acids and organic acid esters, (b) flavonoid, (c) terpenes (d) Others.

From the screening analysis, 34 compounds were characterised from VAL-AB, 21 from VAL-KK, 39 from OGL-AB and 21 from OGL-KK. Altogether 60 compounds were identified in positive mode, and 10 were identified in both negative and positive modes. From the BPI chromatograms (Figures S1 and S2), the positive ionisation mode was better than the negative mode based on the number of compounds ionised and the fragmentation patterns of the identified compounds. The results also showed that both VAL and OGL from Abraka (crude oil-free community) are richer in phytochemicals. These plants have previously reported rich, diverse metabolites [39]. The main chemical compositions identified in this study were various terpenes, flavonoids, and steroids. Interestingly, a handful of compounds unique to VAL-KK and OGL-KK samples collected from Kokori, the crude oil-spill community, were also identified. These compounds are steroids (38, 42) and terpenes (33, 47, 57 and 69). This comprehensive phytochemical profile study revealed the structural diversity of secondary metabolites and matching patterns within VAL and OGL; some similarity was established between VAL and OGL regarding the synthesised compounds. Seven compounds were shared constituents found in all VAL and OGL samples used for this study, irrespective of their collection sites. These are dihydroquercetin (7), caffeic acid (10), linolenic acid (19), isoquercetin (34), rutin (36), *tetranotreterpene* (59) and oleic acid (70). Furthermore, in the nontargeted metabolomic analysis performed and based on the secondary metabolites identified, it was found that there indeed existed differences between VAL-AB and VAL-KK, OGL-AB and OGL-KK, respectively.

For VAL, 13 known metabolites, including eight steroids (31, 33, 38, 42, 44, 53, 57 and 58), two organic acids and organic acid ester (9), one flavonoid (56), two terpenes (47 and 69) and one unknown compound (55) enabling this differentiation were discovered. These compounds were identified only in VAL samples from Kokori, the crude-oil spill community, thereby illustrating the differences between VAL-AB and VAL-KK and, therefore, providing a basis for explaining the effect of different growth environments on secondary sources metabolites. Among these potential biomarkers, compounds 31, 38, 42, 44, 47, 53, 56, and 57 were identified or tentatively characterised in *Vernonia amygdalina* leaves for the first time. As previously stated, a total of 20 compounds were identified in VAL-KK, 13 of which were exclusive to VAL-KK, while the remaining 7 (7, 10, 17, 19, 34, 36 and 70) compounds were identified in both VAL-AB and VAL-KK samples.

With *Ocimum gratissimum* leaves, nine unique compounds (25, 33, 38, 42, 47, 57, 61, 62 and 69) were identified from OGL-KK. These phytochemicals have never been reported in the literature identified or isolated from OGL. Interestingly, some similarity was displayed between samples collected from Kokori, the crude oil-spill community. These metabolites were identified in VAL-KK and OGL-KK; 33, 38, 42, 47, 57 and 69.

3.2. Diversity Evaluation of VAL and OGL Using Metabolomic Analysis

The quality control (QC) samples were clustered tightly within the same quadrant in PCA, suggesting the system's reliability, reproducibility, and stability. Based on their common spectral characteristics, the PCA 2D plots of VAL and OGL samples from crude oil-spill Kokori and crude oil-free Abraka were easily classified within two clusters (Figure 2); they were separated, indicating that samples from Kokori could be easily differentiated from samples from Abraka. The first two components, PC1 and PC2, explained 78.2% and 16.5% of the total variance in the positive mode and 68.2% and 17.2% in the negative mode.

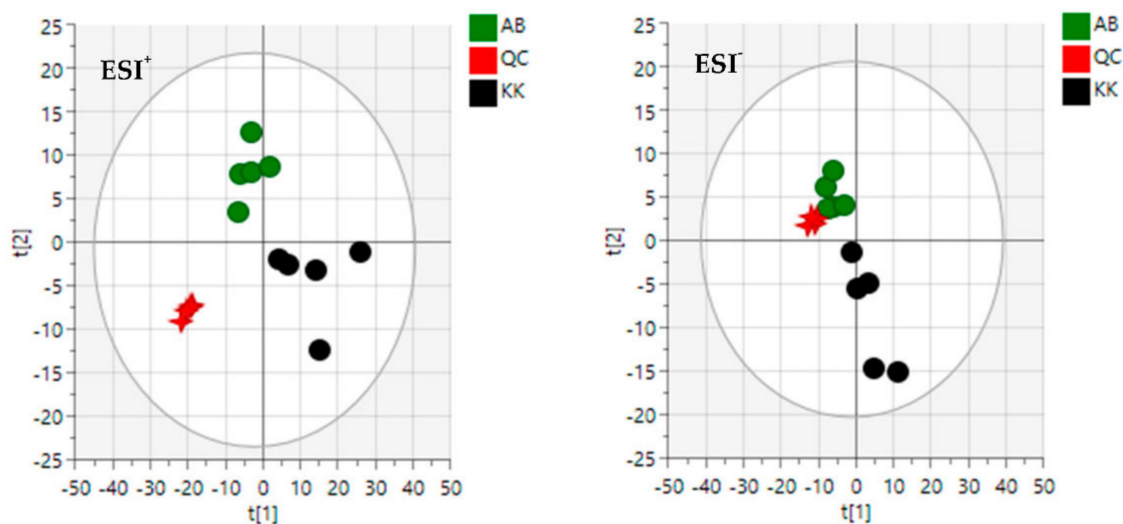


Figure 2. The principal component analysis (PCA) of VAL and OGL in ESI⁺ mode and ESI⁻ mode. AB—Abraka; KK—Kokori; QC—Quality control.

In order to evaluate the variance between the plant samples from the crude oil-spill community (Kokori) and the crude oil-free community (Abraka), the OPLS-DA score plot, permutation test, and variable importance in the projection values were obtained. After OPLS-DA plots (Figures 3a and 4a) in both ESI⁺ and ESI⁻ modes were performed, the maximum separation between the VAL, OGL and, VAK, OGK groups were available.

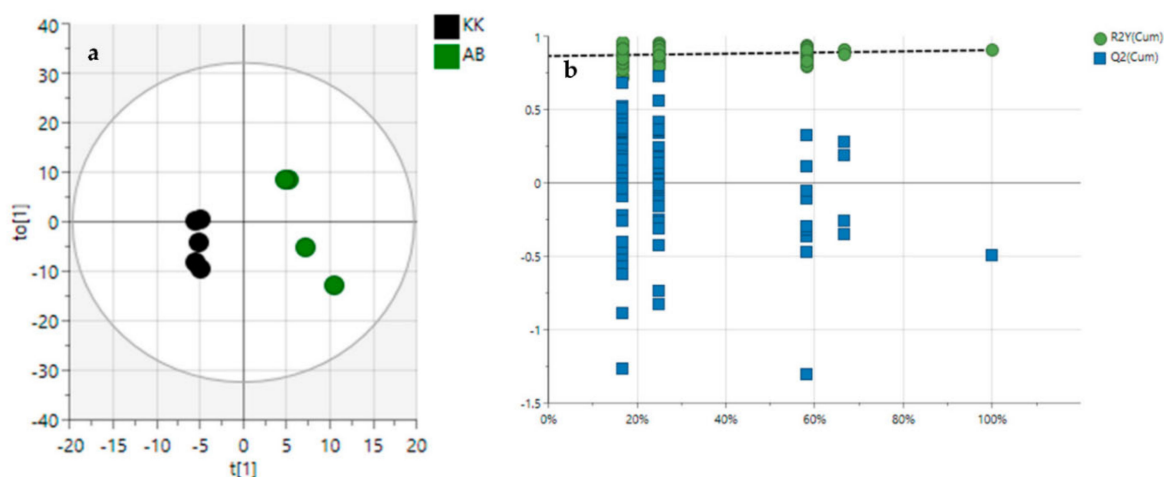


Figure 3. Orthogonal partial least squares discriminant analysis (OPLS-DA) (a), permutation tests, (b) in ESI⁺ mode. AB—Abraka; KK—Kokori.

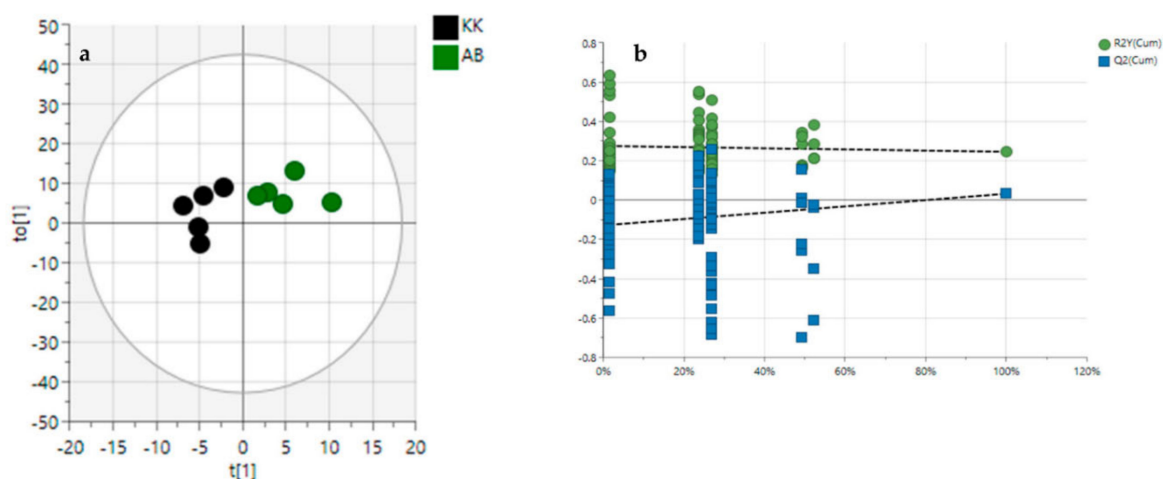


Figure 4. Orthogonal partial least squares discriminant analysis (OPLS-DA) (a), permutation tests, (b) in ESI[−] mode. AB—Abraka; KK—Kokori.

With the permutation testing done, the Q^2 and R^2 values obtained were 0.823 0.721 which suggests that the model can be considered predictive and reproducible. The lines grouping the crude oil-spill and crude oil-free samples were significantly located underneath the random sampling lines (Figures 3b and 4b), indicating a definite validity for the characteristic metabolites identified. Additionally, a heatmap was generated to systematically evaluate the richness of the secondary metabolomes in all the samples (Figure 5); this visualised the metabolite's intensities and diversity in the extracts. Samples were run in triplicates. Multiple blue bands indicate a rich secondary metabolome with a high diversity of metabolites, while fewer blue bands indicate a more limited set of secondary metabolites. The heatmap was also arranged according to the collection sites to investigate the chemical diversity among plant samples from the same species. OGL-AB displayed the richest metabolome of all four extracts.

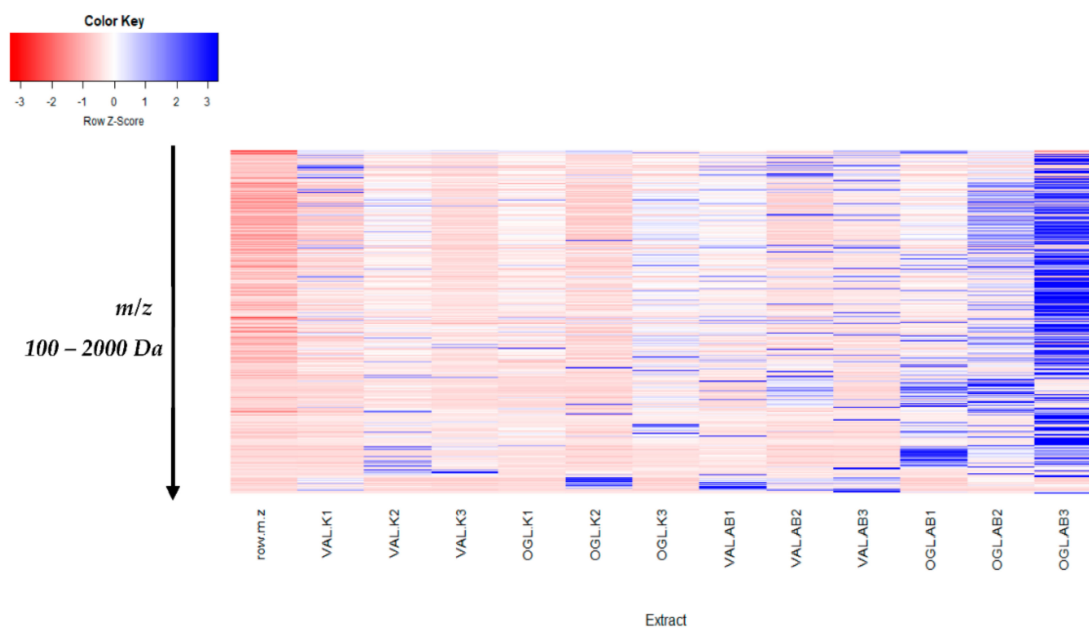


Figure 5. Heatmap visualising the intensities of secondary metabolites. AB—Abraka; KK—Kokori; VAL—*Vernonia amygdalina* leaves; OGL—*Ocimum gratissimum* leaves.

3.3. In Vitro Antisickling Activities of Crude Extracts

Reduction of Sickle cells and Sickling Reversal assay.

The inhibition and reversal of sickling by hydroxyurea (positive standard) and plant extracts (test samples) were conducted to investigate and compare the effect of *Vernonia amygdalina* and *Ocimum gratissimum* extracts collected from the crude oil-rich Kokori and crude oil-free Abraka, Delta State, Nigeria on sickle cell disease. The two study medicinal plants are used within the tribal communities of Abraka and Kokori in Delta state, Nigeria, to manage blood-related diseases such as sickle cell anaemia. The percentage of sickling inhibition and reversal were used in vitro to determine the possible anti-sickling properties of the two plant species on HbSS erythrocytes. Sickle cell disease negatively affects the flexibility of the red blood cell and thus disallows them from their natural kinetic activity with the blood vessels. Antisickling drugs are therefore designed to intrinsically or otherwise prevent or reverse the sickle shape appearance of the red blood cells of HBSS patients. Data obtained from the sickling inhibition experiment and the sickling reversal assay have been presented in Table 3, Figure 6. The effect of the plant extracts was compared with a standard foremost drug, hydroxyurea. Data obtained from this study indicates that the extracts of the two plants possess sickling inhibition (OGL-AB = 28.43%; VAL-AB = 26.89%; OGL-KK = 26.17%; VAL-KK = 26.29%, Hy.urea = 26.36%) (Figure 6) and sickling reversal activities (OGL-AB = 35.31%; VAL-AB = 33.52%; OGL-KK = 29.73%; VAL-KK = 30.22%; Hy.urea = 34.85%) comparable to or marginally higher than the standard drug, hydroxyurea (Table 3). However, in both sickling inhibition and reversal assays, VAL and OGL extract collected from crude oil-free Abraka displayed higher activities than VAL and OGL extracts originating from crude oil spill Kokori; this may be due to the reduction in the number of phytochemicals in the samples from Kokori. As seen in the metabolomic studies (Table S3, Figures 2 and 3), samples collected from crude oil-free Abraka showed a more diverse and richer phytochemical profile than samples from Kokori; this is in agreement with published literature which shows that natural products with richer metabolomes tend to display higher bioactivities [40].

Table 3. Percentage of sickling of erythrocytes treated without extracts (negative control), hydroxyurea (positive control) and with 10 mg/mL extracts.

Samples (Extracts)	% Sickling \pm SD	% Sickling Reversal \pm SD
OGL-AB	28.43 \pm 0.50	35.31 \pm 0.30
VAL-AB	26.89 \pm 0.51	33.52 \pm 0.30
OGL-KK	26.17 \pm 0.16	29.73 \pm 0.12
VAL-KK	26.29 \pm 0.46	30.22 \pm 0.50
Hy.urea	26.36 \pm 0.02	34.85 \pm 0.16
Control	40.25 \pm 0.32	0.00

VAL—*Vernonia amygdalina* leaves from Kokori; OGL-AB—*Ocimum gratissimum* leaves from Abraka; Hy.urea—Hydroxyurea.

The number of cells identified as sickled in the control was over 40%, while in the presence of hydroxyurea, sickling was reduced to 26.36%. Generally, all four extracts tested produced a slight reduction in the number of sickling red blood cells. *Ocimum gratissimum* from Abraka displayed the highest sickling inhibition of 28.43% and sickling reversal of 35.31%. It has previously been reported for its activities against sickling of the HbS [41], while Tshilandi et al. (2015) [2] isolated the bioactive component of the plant and documented ursolic acid as the antisickling agent. Findings from this study are consistent with these reports regarding the antisickling potentials of *Ocimum gratissimum*. *Vernonia amygdalina* has only been reported once [42] for its potentiating activities of polymerisation of red blood cells.

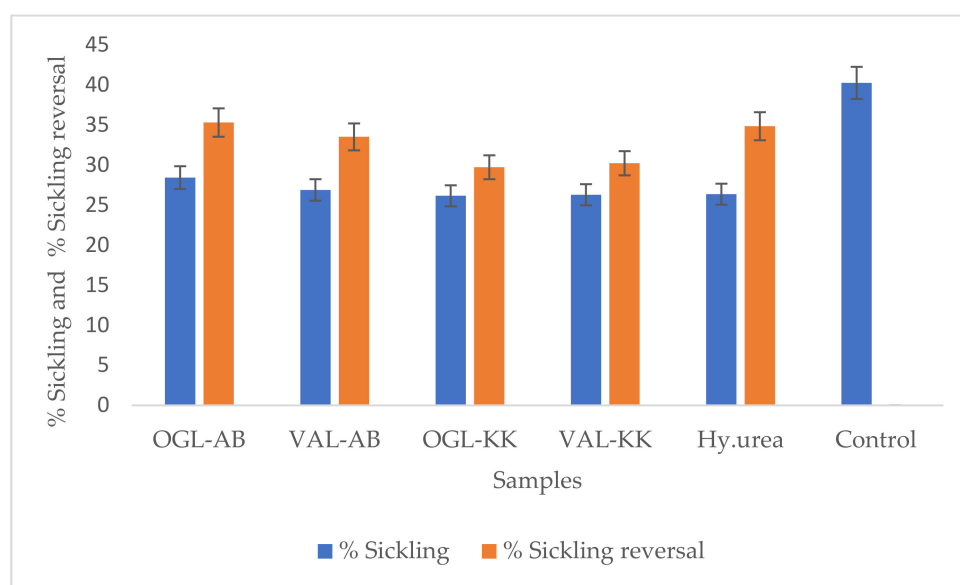


Figure 6. Percentage sickling reduction and sickling reversal of erythrocytes treated with 10 mg/mL extracts. VAL—Vernonia amygdalina leaves from Kokori; OGL-AB—Ocimum gratissimum leaves from Abraka; Hy.urea—Hydroxyurea.

3.4. Structural Elucidation of Compounds Isolated

The methanolic plant extracts, VAL-AB and VAL-KK, were selected for structural elucidation due to their large masses and analysed using HPLC and ^1H NMR. The ^1H NMR showed a wide range of interesting signals that indicated the extract's chemical diversity. The VAL-AB and VAL-KK extracts were fractionated and purified according to the materials and methods. Compound 1, vernodalol [43] was isolated from VAL-AB and VAL-KK, while compound 2, lasiopulide [44] was isolated exclusively from VAL-KK. Both compounds were identified by comparing their experimental NMR and HRESIMS m/z data with published literature (Supplementary Materials).

3.5. Molecular Docking Studies

In recent study, molecular modelling methods have been useful in evaluating the interaction between target molecules and ligands [45]. After identifying the antisickling activities of the crude extracts, the isolated compounds were subjected to virtual screening by molecular docking to predict the interactions between selected target proteins and the molecule and elucidate the possible mechanism of action. Two protein targets, deoxyhemoglobin S (PDB ID: 2HBS) and P-selectin (PDB ID: 1G1S) were obtained from the protein data bank and simulated with vernodalol (compound 1) and lasiopulide (compound 2). The ligands, Protoporphyrin IX and (4R)- 2-Methylpentane-2,4-diol are co-crystallised ligands of deoxyhemoglobin S (PDB ID: 2HBS) and P-selectin (PDB ID: 1G1S), respectively. 4-{2-chloro-4-[3-(1H-imidazol-2-yl)propanoyl]phenoxy}butanoic acid and furfural were also selected for the docking studies, having been previously described to possess antisickling effect via deoxyhaemoglobin and haemoglobin [46,47].

P-selectin is a cellular adhesion receptor that manifests on endothelium and activated platelets and facilitates vaso-occlusion in sickle cell disease (SCD). It modulates the interactions between leukocytes and activated platelets; and participates in the capturing, rolling and recruiting of leukocytes to the activated vascular endothelium. The interaction with platelets triggers the recruitment of monocytes and neutrophils, which promote inflammation [48]. The inhibition of P-selectin has been shown to limit the frequency of vaso-occlusive crises in patients with SCD. Additionally, P-selectin-mutant showed poor leukocyte rolling and retards the leakage of neutrophils to sites of inflammation [49]. An inhibitor that targets P-selectin reduces the pain duration that accompanies

sickle cell crises with a significant reduction in opioid use [50]. Lasiopulide and vernodalol demonstrated a better affinity for the P-selectin receptor (PDB ID: 1G1S) with a binding energy of -20.9200 and -20.7568 kJ/mol, respectively than the co-crystallised ligand ((4R)-2-Methylpentane-2,4-diol) (-15.0624 kJ/mol); this shows the prospect that these phyto-compounds could help in reducing vaso-occlusion in sickle cell disease (SCD) (Figures 7 and 8).

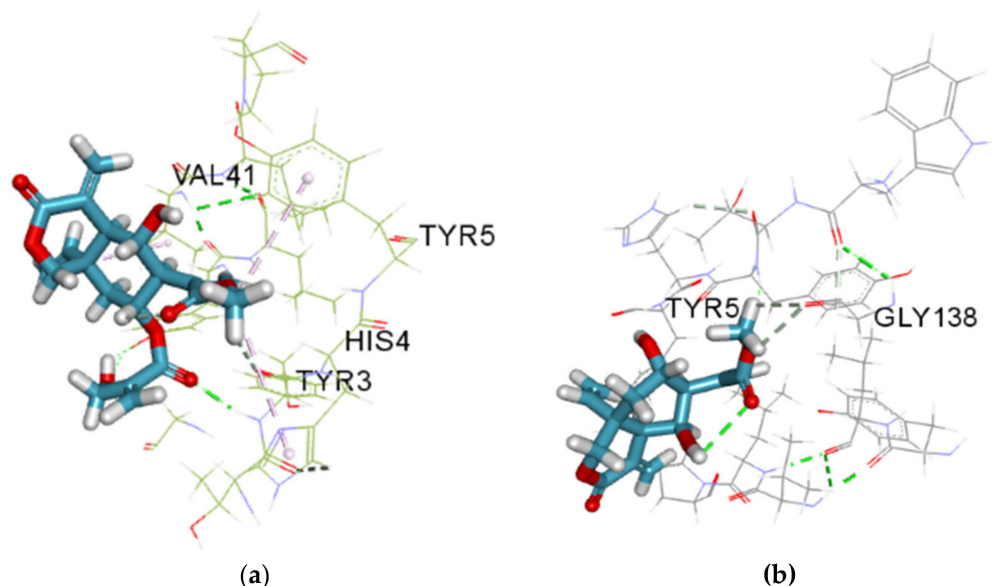


Figure 7. (a) Vernodalol in the active site of P-Selectin (PDB ID: 1G1S). Predicted hydrogen bonding interactions can be seen between vernodalol and active residues VAL 41, TYR5, TYR3 and HIS4. (b) Interaction between lasiopulide and P-selectin (PDB ID: 1G1S). Conventional Hydrogen bond (solid green colour), carbon-hydrogen bond (solid grey colour) and Pi-Alkyl (solid lilac colour).

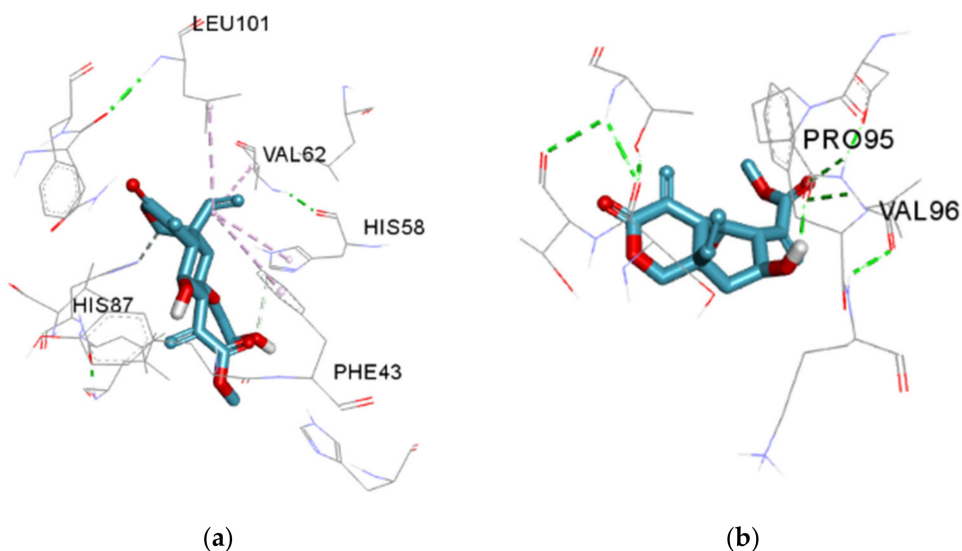


Figure 8. Deoxyhemoglobin S (PDB ID: 2HBS) (a) Lowest energy docked pose of vernodalol (b) Lowest energy docked pose of lasiopulide. Conventional Hydrogen bond (solid green colour), carbon-hydrogen bond (solid grey colour) and Pi-Alkyl (solid lilac colour).

It has been reported that small molecules with a high affinity for HBS or directly modified protein could hinder the polymerisation of this molecule which is the root cause of sickle cell pathology [47]. Agents such as hydroxyurea (HU) currently used in managing and treating SCD may trigger some adverse reactions like myelosuppression. Thus, the search for new antisickling agents is inevitable. Lasiopulide and vernodalol displayed an

affinity for HBS than furfural; a previously reported compound with affinity for HBS [46]; but less than the other co-crystallised ligands (protoporphyrin IX (HEM) and 4-[2-chloro-4-[3-(1H-imidazol-2-yl) propanoyl] phenoxy]butanoic acid (3U8) [47] as shown in Table 4.

Table 4. Docking energies (KJ/mol) of the isolated compounds with target proteins.

Compounds	Binding Affinity (KJ/mol)	
	1G1S	2HBS
Lasiopulide	−20.9200	−23.4304
Vernodalol	−21.7568	−22.5936
(4R)-2-Methylpentane-2,4-diol	−15.0624	−17.9912
Furfural	−13.8072	−16.736
4-[2-chloro-4-[3-(1H-imidazol-2-yl)propanoyl]phenoxy]butanoic acid	NB	−31.7984
Protoporphyrin IX	NB	−43.932

Receptors and PDB ID. 1G1S: P-Selectin; 2HBS: Deoxyhemoglobin S; NB: Non-binding.

The docked structure, vernodalol (Figure 7), exhibited interaction with the active site of P-selectin via TYR3, HIS4, TYR5, and VAL41 residues. This compound demonstrated two H-bond interactions with TYR3, a conventional hydrogen bond and a carbon hydrogen bond, and a pi-alkyl interaction with His4 and TYR5. Docking analysis revealed a Pi-alkyl interaction between lasiopulide and the TYR5 residue and a two-carbon hydrogen bond with the P-Selectin GLY138 residue. According to the results of Vernodalol docking studies with deoxyhemoglobin, a carbon-hydrogen bond exists between the ligand and histidine residue at positions 58 and 87 of the target, while the Pi-alkyl interaction was found with LEU101, VAL62, and PHE43. Lasiopulide with this same target displayed a conventional hydrogen bond with PRO95 and VAL96 and a pi-alkyl interaction with PHE98. P-interactions have been reported to contribute to stabilising binding structures, and the frequency of hydrogen bonds is proportional to strong inhibitor binding. Alkyl and pi-alkyl bonds have also been reported to improve the hydrophobic interaction of the ligand in the binding pocket of the protein [51].

3.6. Pharmacophore Evaluation

Using the lowest energy conformers of vernodalol and lasiopulide, the pharmacophore models were generated [46]. The generated pharmacophore showed three key features: hydrogen bond acceptors (HBAs), hydrogen bond donors (HBDs), and hydrophobic interactions (H). The representative 3D and 2D pharmacophoric features of each compound are shown in Figures 9 and 10. Each compound constitutes individual pharmacophoric features and from these individual characteristic pharmacophores were generated. A merged pharmacophore of vernodalol with common features was generated, as shown in Figure 9. This common feature pharmacophore model of vernodalol with a score of 0.9909 showed certain features: two HBD, five HBAs, and three Hs.

Another merged pharmacophore of lasiopulide with common features was generated, as shown in Figure 10. This common feature pharmacophore model of lasiopulide with a score of 0.9889 showed certain features: two HBD, four HBAs, and two Hs.

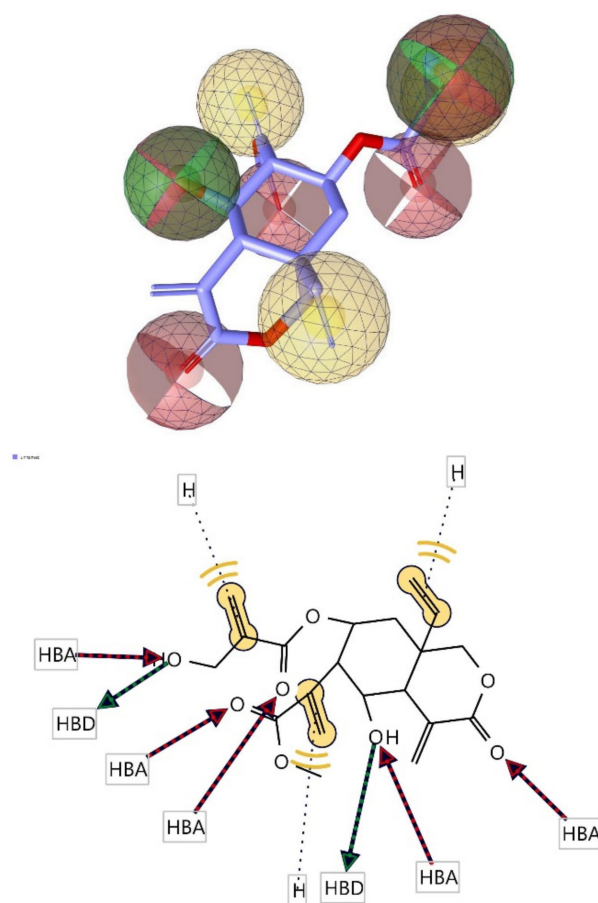


Figure 9. 3D and 2D representations of common pharmacophoric features of vernodalol used in pharmacophore evaluation. Red, HBAs; green, HBDs; Yellow, H; as described earlier.

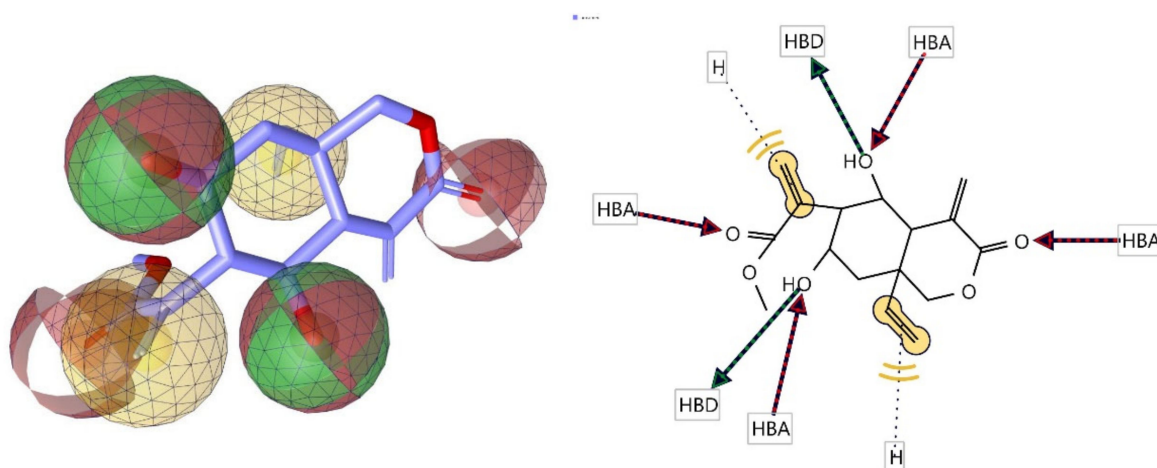


Figure 10. 3D and 2D representations of common pharmacophoric features of lasiopulide used in pharmacophore evaluation. Red, HBAs; green, HBDs; Yellow, H; as described earlier.

4. Conclusions

In this study, the similarity and diversity of phytochemical profile of *Vernonia amygdalina* and *Ocimum gratissimum* samples collected from crude oil-free community (Abraka) and the crude oil-spill community (Kokori) were evaluated. The crude oil-spill community displayed a more prosperous and diverse phytochemical profile than the same samples originating from the crude oil-spill community. The presence of secondary metabolites

such as lasiopulide found exclusively in VAL-KK and OGL-KK strongly supports the hypothesis that the environmental condition induced by crude oil spillage, thus affect the phytochemicals biosynthesis of the plants [52]. Therefore, this may support our assumption that medicinal plants surviving unfavourable crude oil spills may produce potentially new compounds as they adapt to environmental stress.

From the molecular docking studies, vernodalol and lasiopulide displayed an affinity for P-selectin and deoxyhemoglobin S, which are proteins implicated in sickle cell disease; thus, they warrant further investigations such as in vivo and mechanism of action studies. There appears to be a slight difference between the antisickling activities of OGL AND VAL growing in the crude oil-rich Kokori and that growing in crude oil-free Abraka; The impact of the different collection sites on the bioactivities and phytochemical profiles was highlighted by the corresponding differences in chemical profiles and the invitro ant sickling assay. Pharmacophore models were proposed to help guide future drug design studies. Additionally, the proposed pharmacophore models should be used as a future guide for selecting and designing antiparasitic drug candidates. Further studies is therefore warranted to identify and characterise the active phytochemicals present in different active extracts, followed by toxicity analysis and clinical trials.

Supplementary Materials: The following supporting information can be downloaded at: <https://www.mdpi.com/article/10.3390/molecules27238372/s1>, Figure S1. The representative base peak chromatograms (BPC) of VAL and OGL in Electrospray Ionisation (ESI⁺) positive mode; Figure S2. The representative base peak chromatograms (BPC) of VAL and OGL in Electrospray Ionisation (ESI⁻) negative mode; Figure S3. MS data for vernodalol; Figure S4. ¹H NMR spectral of vernodalol; Figure S5. HSQC spectral of vernodalol; Figure S6. COSY spectral of vernodalol; Figure S7. Structures and 2D NMR correlations of vernodalol and lasiopulide (bold: COSY, arrows: HMBC, from H to C); Figure S8. MS of lasiopulide; Figure S9. ¹H NMR of lasiopulide; Figure S10: HSQC spectrum of lasiopulide; Figure S11: COSY spectral of lasiopulide; Table S1. NMR data for vernodalol in CD3OD (400 MHz); Table S2: NMR data for lasiopulide in CD3OD (400 MHz); Table S3. Compounds identified from VAL and OGL by ultra-high-performance liquid chromatography quadrupole time of flight tandem mass spectrometry UPLC-QTOF-MS.

Author Contributions: O.A.D.: Conceptualisation, methodology, funding acquisition, data curation, formal analysis, writing—original draft, review and editing. E.T.O., A.F.A., E.O.O., G.P., S.S. and A.A.F.: formal analysis, methodology, writing—review and editing. A.F.A. and E.O.O.: Raw material acquisition, data curation. E.O.O.: Data curation, raw material acquisition. J.O.M., M.J. and R.E.: Supervision, writing, review and editing. All authors have read and agreed to the published version of the manuscript.

Funding: The authors recognise the financial support of the Schlumberger Faculty for the Future Foundation Scholarship to conduct the present study.

Institutional Review Board Statement: The study was conducted in accordance with the Declaration of Helsinki, and approved by the Ethical Review Committee of the University of Ilorin, Kwara State, Nigeria (UERC Approval Number: UERC/ASN/2022/2352, 15 September 2022) for studies involving human blood.

Informed Consent Statement: Not applicable.

Data Availability Statement: Not applicable.

Acknowledgments: The authors also thank Ruangelie Edrada- Ebel of the Faculty of Pharmaceutical Sciences, The Natural Products Metabolomics Group, Strathclyde Institute of Pharmacy and Biomedical Sciences, University of Strathclyde for her contribution to the methodology.

Conflicts of Interest: The authors have no conflict of interest to declare.

References

1. Gyasi, R.M.; Mensah, C.M.; Adjei, P.; Agyemang, S. Public Perceptions of the Role of Traditional Medicine in the Health Care Delivery System in Ghana. *Glob. J. Health Sci.* **2011**, *3*, 40–49. [\[CrossRef\]](#)
2. Tshilanda, D.D.; Onyamboko, D.N.; Babady-Bila, P.; Ngbolua, K.-T.; Tshibangu, D.S.; Dibwe, E.D.F.; Mpiana, P.T. Anti-sickling Activity of Ursolic Acid Isolated from the Leaves of *Ocimum gratissimum* L. (Lamiaceae). *Nat. Prod. Bioprospecting* **2015**, *5*, 215–221. [\[CrossRef\]](#) [\[PubMed\]](#)
3. Iyare, C.; Uzoigwe, J.; Okorie, P.O.; Ugwu, P.I.; Ezeh, C.O.; Iyare, E.E. Pregnancy outcome and early postnatal weights in diabetic and non-diabetic pregnant rats administered ethanolic extract of *Ocimum gratissimum* leaves during pregnancy. *Int. J. Nurs. Midwifery* **2018**, *10*, 26–32. [\[CrossRef\]](#)
4. Maud, K.M.; Hannington, O.O.; Olwa, O.; Dominic, W.M. Ethno-pharmacological screening of *Vernonia amygdalina* and *Cleome gynandra* traditionally used in Childbirth in Western Uganda. In Proceedings of the 11th NAPRECA Symposium Book of Proceedings, Antananarivo, Madagascar, 9–12 August 2005.
5. Adedayo, L.D.; Seun, G. Anxiolytic and explorative potentials of the methanol leaf extract of *Vernonia amygdalina* in male Wistar rats. *Ann. Depress. Anxiety-Vol.* **2018**, *5*, 1094. [\[CrossRef\]](#)
6. Ofem, O.; Ani, E.; Eno, A. Effect of aqueous leaves extract of *Ocimum gratissimum* on hematological parameters in rats. *Int. J. Appl. Basic Med. Res.* **2012**, *2*, 38–42. [\[CrossRef\]](#)
7. Oyeyemi, I.T.; Akinlabi, A.A.; Adewumi, A.; Aleshinloye, A.O.; Oyeyemi, O.T. *Vernonia amygdalina*: A folkloric herb with anthelmintic properties. *Beni-Suef Univ. J. Basic Appl. Sci.* **2018**, *7*, 43–49. [\[CrossRef\]](#)
8. Nabukenya, I.; Rubaire-Akiiki, C.; Olila, D.; Ikwap, K.; Höglund, J. Ethnopharmacological practices by livestock farmers in Uganda: Survey experiences from Mpigi and Gulu districts. *J. Ethnobiol. Ethnomedicine* **2014**, *10*, 9. [\[CrossRef\]](#)
9. Adeniyi, S.A.; Orjiokwe, C.L.; Ehiagbonare, J.E.; Arimah, B.D. Preliminary phytochemical analysis and insecticidal activity of ethanolic extracts of four tropical plants (*Vernonia amygdalina*, *Sida acuta*, *Ocimum gratissimum* and *Telfaria occidentalis*) against beans weevil (*Acanthscelides obtectus*). *Int. J. Phys. Sci.* **2010**, *5*, 753–762.
10. Okon, U.A.; Umoren, I.U. Comparison of antioxidant activity of insulin, *Ocimum gratissimum* L. and *Vernonia amygdalina* L. in type 1 diabetic rat model. *J. Integr. Med.* **2017**, *15*, 302–309. [\[CrossRef\]](#)
11. Kadiri, O.; Olawoye, B. *Vernonia amygdalina*: An underutilized vegetable with nutraceutical Potentials—A Review. *Turk. J. Agric. Food Sci. Technol.* **2016**, *4*, 763–768. [\[CrossRef\]](#)
12. Mgbeje, B.I.; Umoh, E.U.; Emmanuel-Ikpeme, C. Comparative analysis of phytochemical composition of four selected tropical medicinal plants namely: *Ocimum gratissimum*, *Piper guineense*, *Gongronema latifolium* and *Vernonia amygdalina*. *J. Complement. Altern. Med. Res.* **2019**, *7*, 1–11. [\[CrossRef\]](#)
13. Diyaolu, O.A.; Attah, A.F.; Oluwabusola, E.T.; Moody, J.O.; Jaspars, M.; Ebel, R. Heavy Metals, Proximate Analysis and Brine Shrimp Lethality of *Vernonia amygdalina* and *Ocimum gratissimum* Growing in Crude Oil-Rich Delta State, Nigeria. *Foods* **2021**, *10*, 2913. [\[CrossRef\]](#) [\[PubMed\]](#)
14. Agbogidi, O. Trace metal profile of some fruits in Kokori and Abraka Market, Delta State, Nigeria. *Int. J. Sch. Res. Gate* **2014**, *2*, 4.
15. Rees, D.C.; Williams, T.N.; Gladwin, M.T. Sick-cell disease. *Lancet* **2010**, *376*, 2018–2031. [\[CrossRef\]](#) [\[PubMed\]](#)
16. Ingram, V.M. Gene mutations in human haemoglobin: The chemical difference between normal and sickle cell haemoglobin. *Nature* **1957**, *180*, 326–328. [\[CrossRef\]](#)
17. Nurain, I.O.; Bewaji, C.O.; Johnson, J.S.; Davenport, R.D.; Zhang, Y. Potential of Three Ethnomedicinal Plants as Antisickling Agents. *Mol. Pharm.* **2017**, *14*, 172–182. [\[CrossRef\]](#)
18. Vichinsky, E.; Hoppe, C.C.; Ataga, K.I.; Ware, R.E.; Nduba, V.; El-Beshlawy, A.; Hassab, H.; Achebe, M.M.; Alkindi, S.; Brown, R.C.; et al. A Phase 3 Randomized Trial of Voxelotor in Sickle Cell Disease. *N. Engl. J. Med.* **2019**, *381*, 509–519. [\[CrossRef\]](#)
19. Piel, F.B.; Hay, S.I.; Gupta, S.; Weatherall, D.J.; Williams, T.N. Global burden of sickle cell anaemia in children under five, 2010–2050: Modelling based on demographics, excess mortality, and interventions. *PLoS Med.* **2013**, *10*, e1001484. [\[CrossRef\]](#)
20. Lasch, J.; Küllertz, G.; Opalka, J.R. Separation of Erythrocytes into Age-Related Fractions by Density or Size? Counterflow Centrifugation. *Clin. Chem. Lab. Med. (CCLM)* **2000**, *38*, 629–632. [\[CrossRef\]](#)
21. Agrawal, R.K.; Patel, R.K.; Nainiwal, L.; Trivedi, B. Hydroxyurea in sickle cell disease: Drug review. *Indian J. Hematol. Blood Transfus.* **2014**, *30*, 91–96. [\[CrossRef\]](#)
22. Niihara, Y.; Miller, S.T.; Kanter, J.; Lanzkron, S.; Smith, W.R.; Hsu, L.L.; Vichinsky, E.P. A phase 3 trial of l-glutamine in sickle cell disease. *N. Engl. J. Med.* **2018**, *379*, 226–235. [\[CrossRef\]](#)
23. Ataga, K.I.; Kutlar, A.; Kanter, J.; Liles, D.; Cancado, R.; Friedrisch, J.; Guthrie, T.H.; Knight-Madden, J.; Alvarez, O.A.; Gordeuk, V.R.; et al. Crizanlizumab for the Prevention of Pain Crises in Sickle Cell Disease. *N. Engl. J. Med.* **2017**, *376*, 429–439. [\[CrossRef\]](#)
24. Herity, L.B.; Vaughan, D.M.; Rodriguez, L.R.; Lowe, D.K. Voxelotor: A Novel Treatment for Sickle Cell Disease. *Ann. Pharmacother.* **2021**, *55*, 240–2451. [\[CrossRef\]](#)
25. Wang, C.; Zhang, N.; Wang, Z.; Qi, Z.; Zhu, H.; Zheng, B.; Li, P.; Liu, J. Nontargeted Metabolomic Analysis of Four Different Parts of *Platycodon grandiflorum* Grown in Northeast China. *Molecules* **2017**, *22*, 1280. [\[CrossRef\]](#)
26. Wang, Y.; Wang, C.; Lin, H.; Liu, Y.; Li, Y.; Zhao, Y.; Li, P.; Liu, J. Discovery of the Potential Biomarkers for Discrimination between *Hedyotis diffusa* and *Hedyotis corymbosa* by UPLC-QTOF/MS Metabolome Analysis. *Molecules* **2018**, *23*, 1525. [\[CrossRef\]](#)
27. Adusumilli, R.; Mallick, P. Data Conversion with ProteoWizard msConvert. *Methods Mol. Biol.* **2017**, *1550*, 339–368.

28. Pluskal, T.; Castillo, S.; Villar-Briones, A.; Orešič, M. MZmine 2: Modular framework for processing, visualizing, and analyzing mass spectrometry-based molecular profile data. *BMC Bioinform.* **2010**, *11*, 395. [[CrossRef](#)]
29. Pang, Z.; Wang, G.; Ran, N.; Lin, H.; Wang, Z.; Guan, X.; Yuan, Y.; Fang, K.; Liu, J.; Wang, F. Inhibitory Effect of Methotrexate on Rheumatoid Arthritis Inflammation and Comprehensive Metabolomics Analysis Using Ultra-Performance Liquid Chromatography-Quadrupole Time of Flight-Mass Spectrometry (UPLC-Q/TOF-MS). *Int. J. Mol. Sci.* **2018**, *19*, 2894. [[CrossRef](#)]
30. Triba, M.N.; Le Moyec, L.; Amathieu, R.; Goossens, C.; Bouchemal, N.; Nahon, P.; Rutledge, D.N.; Savarin, P. PLS/OPLS models in metabolomics: The impact of permutation of dataset rows on the K-fold cross-validation quality parameters. *Mol. Biosyst.* **2015**, *11*, 13–19. [[CrossRef](#)]
31. Pauline, N.; Cabral, B.N.P.; Anatole, P.C.; Jocelyne, A.M.V.; Bruno, M.; Jeanne, N.Y. The in vitro antisickling and antioxidant effects of aqueous extracts *Zanthoxylum heitzii* on sickle cell disorder. *BMC Complement. Altern. Med.* **2013**, *13*, 162. [[CrossRef](#)]
32. Harrington, D.J.; Adachi, K.; Royer, W.E., Jr. The high resolution crystal structure of deoxyhemoglobin S. *J. Mol. Biol.* **1997**, *272*, 398–407. [[CrossRef](#)] [[PubMed](#)]
33. Somers, W.S.; Tang, J.; Shaw, G.D.; Camphausen, R.T. Insights into the molecular basis of leukocyte tethering and rolling revealed by structures of P- and E-selectin bound to SLeX and PSGL-1. *Cell* **2000**, *103*, 467–479. [[CrossRef](#)] [[PubMed](#)]
34. Pettersen, E.F.; Goddard, T.D.; Huang, C.C.; Couch, G.S.; Greenblatt, D.M.; Meng, E.C.; Ferrin, T.E. UCSF Chimera—A visualization system for exploratory research and analysis. *J. Comput. Chem.* **2004**, *25*, 1605–1612. [[CrossRef](#)] [[PubMed](#)]
35. Shapovalov, M.V.; Dunbrack, R.L. A Smoothed Backbone-Dependent Rotamer Library for Proteins Derived from Adaptive Kernel Density Estimates and Regressions. *Structure* **2011**, *19*, 844–858. [[CrossRef](#)] [[PubMed](#)]
36. Dallakyan, S.; Olson, A.J. Small-molecule library screening by docking with pyrX. *Methods Mol. Biol.* **2015**, *1263*, 243–250.
37. Koul, J.L.; Koul, S.; Singh, C.; Taneja, S.C.; Shanmugavel, M.; Kampasi, H.; Qazi, G.N. In vitro cytotoxic elemanolides from *Vernonia lasiopos*. *Planta Med.* **2003**, *69*, 164–166. [[CrossRef](#)]
38. Wolber, G.; Thierry, L. LigandScout: 3-D pharmacophores derived from protein-bound ligands and their use as virtual screening filters. *J. Chem. Inf. Model* **2005**, *45*, 160–169. [[CrossRef](#)]
39. Jisaka, M.; Ohigashi, H.; Takegawa, K.; Hirota, M.; Irie, R.; Huffman, M.A.; Koshimizu, K. Steroid glucosides from *Vernonia amygdalina*, a possible chimpanzee medicinal plant. *Phytochemistry* **1993**, *34*, 409–413. [[CrossRef](#)]
40. Heavisides, E.; Rouger, C.; Reichel, A.F.; Ulrich, C.; Wenzel-Storjohann, A.; Sebens, S.; Tasdemir, D. Seasonal variations in the metabolome and bioactivity profile of *Fucus vesiculosus* extracted by an optimised, pressurised liquid extraction protocol. *Mar. Drugs* **2018**, *16*, 503. [[CrossRef](#)]
41. Alabi, Q.K.; Akomolafe, R.O.; Omole, J.G.; Aturamu, A.; Ige, M.S.; Kayode, O.O.; Kajewole-Alabi, D. Polyphenol-rich extract of *Ocimum gratissimum* leaves prevented toxic effects of cyclophosphamide on the kidney function of Wistar rats. *BMC Complement. Med. Ther.* **2021**, *21*, 274. [[CrossRef](#)]
42. Chikezie, P. Studies on the anti-sickling effects of *Azadirachta indica* and *Vernonia amygdalina* on Hbss erythrocytes. *Int. J. Nat. Appl. Sci.* **2006**, *2*, 24–28. [[CrossRef](#)]
43. Li, X.J.; Zhang, Q.; Zhang, A.L.; Gao, J.M. Metabolites from *Aspergillus fumigatus*, an endophytic fungus associated with *Melia azedarach*, and their antifungal, antifeedant, and toxic activities. *J. Agric. Food Chem.* **2012**, *60*, 3424–3431. [[CrossRef](#)]
44. Copmans, D.; Rateb, M.; Tabudravu, J.N.; Pérez-Bonilla, M.; Dirckx, N.; Vallorani, R.; Diaz, C.; del Palacio, J.P.; Smith, A.J.; Ebel, R.; et al. Zebrafish-Based Discovery of Antiseizure Compounds from the Red Sea: Pseurotin A₂ and Azaspirofurane A. *ACS Chem. Neurosci.* **2018**, *9*, 1652–1662. [[CrossRef](#)]
45. Alberto, A.V.P.; Ferreira, N.C.D.S.; Soares, R.F.; Alves, L.A. Molecular Modeling Applied to the Discovery of New Lead Compounds for P2 Receptors Based on Natural Sources. *Front. Pharmacol.* **2020**, *11*, 01221. [[CrossRef](#)]
46. Safo, M.K.; Abdulmalik, O.; Danso-Danquah, R.; Burnett, J.C.; Nokuri, S.; Joshi, G.S.; Musayev, F.N.; Asakura, T.; Abraham, D.J. Structural Basis for the Potent Antisickling Effect of a Novel Class of Five-Membered Heterocyclic Aldehydic Compounds. *J. Med. Chem.* **2004**, *47*, 4665–4676. [[CrossRef](#)]
47. Omar, A.M.; Mahran, M.A.; Ghatge, M.S.; Chowdhury, N.; Bamane, F.H.A.; El-Araby, M.E.; Abdulmalik, O.; Safo, M.K. Identification of a novel class of covalent modifiers of hemoglobin as potential antisickling agents. *Org. Biomol. Chem.* **2015**, *13*, 6353–6370. [[CrossRef](#)]
48. Wagner, D.D.; Frenette, P.S. The vessel wall and its interactions. *Blood J. Am. Soc. Hematol.* **2008**, *111*, 5271–5281. [[CrossRef](#)]
49. Mayadas, T.N.; Johnson, R.C.; Rayburn, H.; Hynes, R.O.; Wagner, D.D. Leukocyte rolling and extravasation are severely compromised in P selectin-deficient mice. *Cell* **1993**, *74*, 541–554. [[CrossRef](#)]
50. Telen, M.J.; Wun, T.; McCavit, T.L.; De Castro, L.M.; Krishnamurti, L.; Lanzkron, S.; Hsu, L.L.; Smith, W.R.; Rhee, S.; Magnani, J.L.; et al. Randomized Phase 2 Study of GMI-1070 in SCD: Reduction in Time to Resolution of Vaso-Occlusive Events and Decreased Opioid Use. *Blood* **2015**, *125*, 2656–2664. [[CrossRef](#)]
51. Patil, R.; Das, S.; Stanley, A.; Yadav, L.; Sudhakar, A.; Varma, A.K. Optimized Hydrophobic Interactions and Hydrogen Bonding at the Target-Ligand Interface Leads the Pathways of Drug-Designing. *PLoS ONE* **2010**, *5*, e12029. [[CrossRef](#)]
52. Li, Y.; Kong, D.; Fu, Y.; Sussman, M.R.; Wu, H. The effect of developmental and environmental factors on secondary metabolites in medicinal plants. *Plant Physiol. Biochem.* **2020**, *148*, 80–89. [[CrossRef](#)] [[PubMed](#)]